nature chemistry

Article

https://doi.org/10.1038/s41557-024-01666-y

Protocells by spontaneous reaction of cysteine with short-chain thioesters

Received: 16 February 2024

Accepted: 7 October 2024

Published online: 30 October 2024

Check for updates

Christy J. Cho[1,5], Taeyang An[1,5], Yei-Chen Lai[2,3,4], Alberto Vázquez-Salazar[2], Alessandro Fracassi[1], Roberto J. Brea[1], Irene A. Chen[2,3] & Neal K. Devaraj[1]

All known forms of life are composed of cells, whose boundaries are defined by lipid membranes that separate and protect cell contents from the environment. It is unknown how the earliest forms of life were compartmentalized. Several models have suggested a role for single-chain lipids such as fatty acids, but the membranes formed are often unstable, particularly when made from shorter alkyl chains ($\leq C_8$) that were probably more prevalent on prebiotic Earth. Here we show that the amino acid cysteine can spontaneously react with two short-chain (C_8) thioesters to form diacyl lipids, generating protocell-like membrane vesicles. The three-component reaction takes place rapidly in water using low concentrations of reactants. Silica can catalyse the formation of protocells through a simple electrostatic mechanism. Several simple aminothiols react to form diacyl lipids, including short peptides. The protocells formed are compatible with functional ribozymes, suggesting that coupling of multiple short-chain precursors may have provided membrane building blocks during the early evolution of cells.

All life on Earth requires lipid membranes, which separate the interior of cells from the extracellular environment, control transport and act as a scaffold for numerous biochemical reactions. Given their importance in biology, it has long been questioned what constituted the very first, primordial cell membrane-like structures on Earth before the emergence of life, and how such structures could have been formed in the absence of complex and highly evolved biological machinery? In extant cells, the membrane is predominantly composed of phospholipids[1]. Phospholipids have complex chemical structures, consisting of two hydrophobic tails connected to a polar head group, and their biosynthesis requires a multistep enzymatic process that utilizes several soluble and membrane-bound proteins[2,3]. Thus, it is unlikely that diacyl phospholipids were the primary constituents of the earliest membranes found in protocells. The first protocell membranes could have instead formed from substances that were either abundant on the early Earth or were derived from much simpler precursors through spontaneous chemical reactions[4–8].

Fatty acids have been shown to be generated under prebiotically plausible conditions and have also been found in certain meteorites, suggesting that fatty acids were probably present on early Earth[9–13]. Non-enzymatic fatty acid synthesis results in predominantly short-chain species, with chain lengths below ten carbons[11–14]. Although past studies have shown that fatty acids present in some meteorites can form membrane-bound structures[15], due to the presence of a single hydrophobic tail, only long-chain fatty acids ($>C_{12}$) can efficiently assemble into membrane structures at low millimolar concentrations[16–18]. There is therefore an apparent paradox; short-chain fatty acids can be generated more abundantly under abiotic conditions, but longer-chain fatty acids can efficiently assemble into membranes at low concentrations. Furthermore, fatty acid membranes are only stable within a narrow pH range (around their pK_a value) and are unstable in the presence of divalent cations such as Mg^{2+} and Ca^{2+}, which are required for evolution of more advanced biochemical structures such as functional ribozymes[19,20]. For these reasons and others, it is unlikely

[1]Department of Chemistry and Biochemistry, University of California, San Diego, La Jolla, CA, USA. [2]Department of Chemical and Biomolecular Engineering, University of California, Los Angeles, Los Angeles, CA, USA. [3]Department of Chemistry and Biochemistry, University of California, Los Angeles, Los Angeles, CA, USA. [4]Present address: Department of Chemistry, National Chung Hsing University, Taichung City, Taiwan. [5]These authors contributed equally: Christy J. Cho, Taeyang An. e-mail: ndevaraj@ucsd.edu

https://doi.org/10.1038/s41557-024-01666-y

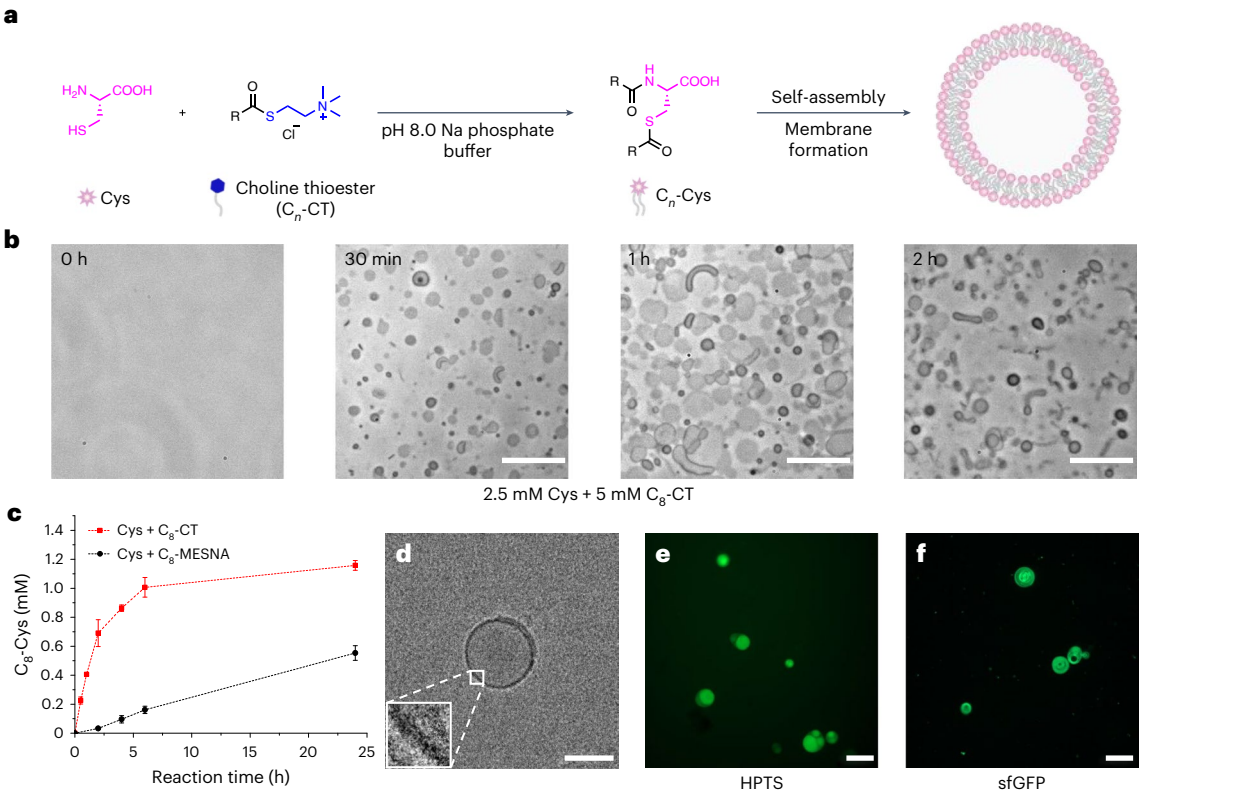

Fig. 1 | Vesicle formation by reaction of cysteine with choline thioesters. **a**, Schematic showing the diacylation of cysteine and in situ self-assembly of vesicles. **b**, Phase-contrast microscopy images of the reaction mixture of 2.5 mM Cys and 5 mM C_8-CT in 0.1 M, pH 8.0 sodium phosphate buffer at the indicated time points. Scale bars, 25 µm. **c**, Reaction kinetics of the diacylation between 2.5 mM Cys and 5 mM C_8 thioesters. The product was quantified by LCMS using 230 nm absorbance. The data points are presented as means ± s.d. ($n = 3$ technically independent samples). **d**, Cryogenic electron microscopy image of a representative C_8-Cys vesicle. Inset: a magnified image (5×) of a selected area in **d**. Scale bar, 50 nm. **e**,**f**, Fluorescence microscopy images of 0.5 mM C_8-Cys vesicles containing 1 mM 8-hydroxypyrene-1,3,6-sulfonic acid (HPTS) (**e**) or 5 µM superfolder green fluorescent protein (sfGFP) in 0.1 M, pH 8.0 sodium phosphate buffer (**f**). Scale bars, 25 µm.

that the first protocellular membranes consisted solely of single-chain fatty acids.

Although several studies have observed stabilizing effects using mixed membranes[13,19–24], an intriguing alternative is that chemical reactions between simple and abundant molecules could have led to the generation of more complex amphiphilic species. In this scenario, a non-enzymatic protometabolism would be required to generate lipid species that would then spontaneously assemble to form a closed membrane-bound protocell. In this context, various amphiphiles have been suggested to address the limitations of fatty-acid-based vesicles[13]. For example, it was reported that dipolyprenylphosphate and dipolyprenylpyrophosphates can form vesicles with C_{10} hydrophobic tails[25,26] and photodimerization of 2-oxocarboxylic acids was shown to generate lipid structures[27]. More recently, cyclophospholipids with C_9 tails were found to form vesicles[28]. Furthermore, diacylglycerol phosphate with two C_8 tails produces vesicle structures[29] and diacylglycerol phosphate amphiphiles bearing longer C_{10} tails were detected using a prebiotically plausible wet–dry cycle[28,30]. Despite these advances, previous models have potential limitations, such as high critical aggregation concentration of the lipid species[28], the need for organic cosolvents for amphiphile synthesis[29] or the simultaneous presence of multiple chemical species, including phosphate sources at very high concentrations[28,30]. The ability to maintain biochemical reactions inside vesicles formed from such lipids has also been underexplored. There would therefore be considerable interest in exploring new vesicle-forming amphiphiles generated in situ via a spontaneous reaction between simple reactive precursors under dilute conditions, as well as determining whether the vesicles formed can sustain internal biochemical reactions.

We had previously reported that a cysteine (Cys)-functionalized lysophosphatidylcholine lipid undergoes native chemical ligation with sodium 2-mercaptoethane sulfonate (MESNA) thioesters to produce non-canonical phospholipids[31,32]. Interestingly, it was also observed that the remaining thiol group of the diacylated product can further react with additional thioesters to generate phospholipids containing three alkyl chains. Inspired by these findings, we hypothesized that cysteine itself may undergo native chemical ligation in the presence of acyl thioesters followed by substrate reloading, leading to the production of diacylcysteine species. Both cysteine and short-chain thioesters have been shown to be synthesized by prebiotically plausible routes, and both can be produced in abundance, the latter through derivatization of short-chain fatty acids[33,34]. Furthermore, recent studies have highlighted the importance of cysteine in prebiotic metabolism, for instance, as a catalyst for peptide bond formation[33]. Considering the smaller head group size of the diacylcysteines compared to conventional phospholipids, and the presence of two hydrophobic tails, we suspected that diacylcysteines would have a much lower critical aggregation concentration compared with single-chain fatty acids of similar tail lengths, which may enable vesicle formation even with very short-chain thioester precursors.

Here we report the spontaneous diacylation of Cys with short-chain choline thioesters, forming cell-like giant membrane vesicles (Fig. 1a). Diacylcysteine compounds with very short C_8 hydrophobic tails form lamellar vesicle structures at submillimolar concentrations, probably because the compact head group has a comparable cross-sectional area to the two short hydrophobic tails. We find that the formation of diacylcysteine protocells was facilitated by silica substrates, supporting previous models of primordial membrane assembly[35].

https://doi.org/10.1038/s41557-024-01666-y

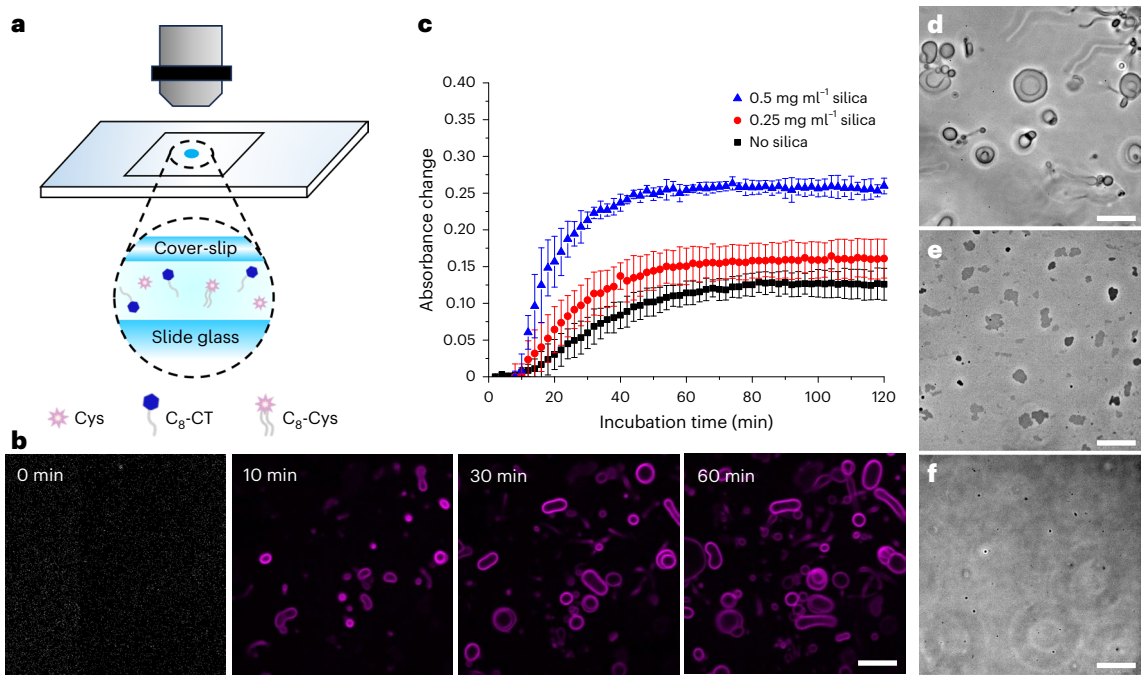

Fig. 2 | Effect of the silica surface on formation of diacylcysteine vesicles. **a**, Schematic illustration of the microscopy set-up for observing the in situ formation of C_8-Cys vesicles on a silica substrate. **b**, Fluorescence microscopy images showing the formation of the C_8-Cys vesicles on the glass cover-slip at various time points. The reaction was conducted using 1 mM Cys and 2 mM C_8-CT in 0.1 M sodium phosphate buffer at pH 8.0 containing 0.5 µM Nile Red as a membrane-staining dye (pseudo-colour change from red to magenta). Scale bar, 10 µm. **c**, Turbidity change during formation of C_8-Cys vesicles with or without silica microspheres. The reaction was conducted using 1 mM Cys and 2 mM C_8-CT in 0.1 M sodium phosphate buffer at pH 8.0 in polystyrene cuvettes. The absorbance was measured at 400 nm. The product was quantified by LCMS using the absorbance at 230 nm. The data points are presented as means ± s.d. ($n = 3$ technically independent samples). **d**–**f**, Representative phase-contrast microscopy images of in situ C_8-Cys vesicle formation with 1 mM Cys and 2 mM C_8-CT on bare glass (**d**), APTES-modified glass (**e**) and C_{18}-modified glass (**f**). The images were obtained after 2 h of incubation. Scale bars, 25 µm.

We propose a simple electrostatic mechanism for substrate-templated membrane formation and describe several experiments that support our hypothesis. Accumulation of lipids at the mineral surface results in the formation of diacylcysteine vesicles at concentrations far lower than the critical aggregation concentration. Unlike fatty acids, and even phospholipids, the head group of the lipid can be varied dramatically by diacylation of *N*-terminal Cys-containing peptides. This suggests the potential for susbtantial structural diversity and functionality in primordial membranes containing lipopeptides. Finally, we demonstrate that membrane-bound vesicles formed from simple diacylated cysteines are resistant to divalent cations, allowing simple biochemical reactions mediated by ribozymes to take place internally.

Results and discussion

Generation of diacylcysteine vesicles and their characterization

Initial reactions were performed using Cys and two different short-chain thioesters, C_8-MESNA and C_8-CT (Supplementary Fig. 1). Thioesters can be produced by condensation between carboxylic acids and thiols. We previously demonstrated synthesis of a choline thioester from oleic acid and thiocholine in aqueous conditions using dicyanamide—a prebiotically available condensation agent[34,36]. We also confirmed that C_8-CT can be produced from octanoic acid and thiocholine under similar reaction conditions (Supplementary Fig. 2). Reactions were performed in glass vials by mixing 2.5 mM Cys with 5 mM C_8 thioesters in 0.1 M, pH 8.0 sodium phosphate buffer at room temperature. Diacylation products (C_8-Cys) were detected by liquid chromatography–mass spectrometry (LCMS) (Fig. 1c), and the formation of the vesicles was clearly observed through phase-contrast microscopy using either of the thioester precursors; however, product and vesicle formation was much faster when C_8-CT was used (Fig. 1b and Supplementary Fig. 3). During the reaction between Cys and C_8-CT, large vesicular structures observable by light microscopy appeared within 30 min of incubation. As expected, incubation of only Cys or C_8-CT did not yield any vesicle structures under similar conditions (Supplementary Fig. 4). The reaction between Cys and C_8-CT favoured the formation of diacylated product over the monoacylated species even at the initial stages of the reaction or when substoichiometric quantities of C_8-CT were used, probably due to faster secondary acylation of the free thiol due to interactions between the hydrophobic tails of the monoacylated species and C_8-CT, which could position the species in close proximity within mixed micelles[37,38].

Cryogenic electron microscopy (cryo-EM) analysis of C_8-Cys vesicles revealed a membrane thickness of 2.62 ± 0.06 nm—approximately twice the length of a single C_8-Cys molecule, suggesting that the membranes formed by C_8-Cys possess a bilayer structure (Fig. 1d). To probe the stability of the vesicles formed, the critical aggregation concentration of C_8-Cys was evaluated using the solvatochromic dye Laurdan. C_8-Cys exhibited a critical aggregation concentration of 0.9 mM, which is much lower than the critical aggregation concentration of short-chain carboxylic acids such as octanoic acid (critical aggregation concentration = 250 mM)[18] and even longer-chain carboxylic-acid-like myristoleic acid (critical aggregation concentration = 4 mM)[16] (Supplementary Fig. 8a). Since the critical aggregation concentration of simple amphiphiles tends to decrease exponentially as the number of carbon atoms in the hydrophobic portion of the molecule increases, the much lower critical aggregation concentration of diacylcysteine compared to single-chain fatty acids could be attributed to the presence of two fatty tails[13,18]. It is notable that large vesicle structures can be readily formed from relatively low concentrations of C_8-Cys. Past work has shown that light-induced dimerization of 2-oxooctanoic acid forms colloidal structures at concentrations above 6 mM (ref. 27); however, whether such species form true vesicles was not explored. It has been reported that diacylglycerol phosphate with C_8 hydrophobic tails can form vesicles at a critical aggregation concentration of 4.55 mM

https://doi.org/10.1038/s41557-024-01666-y

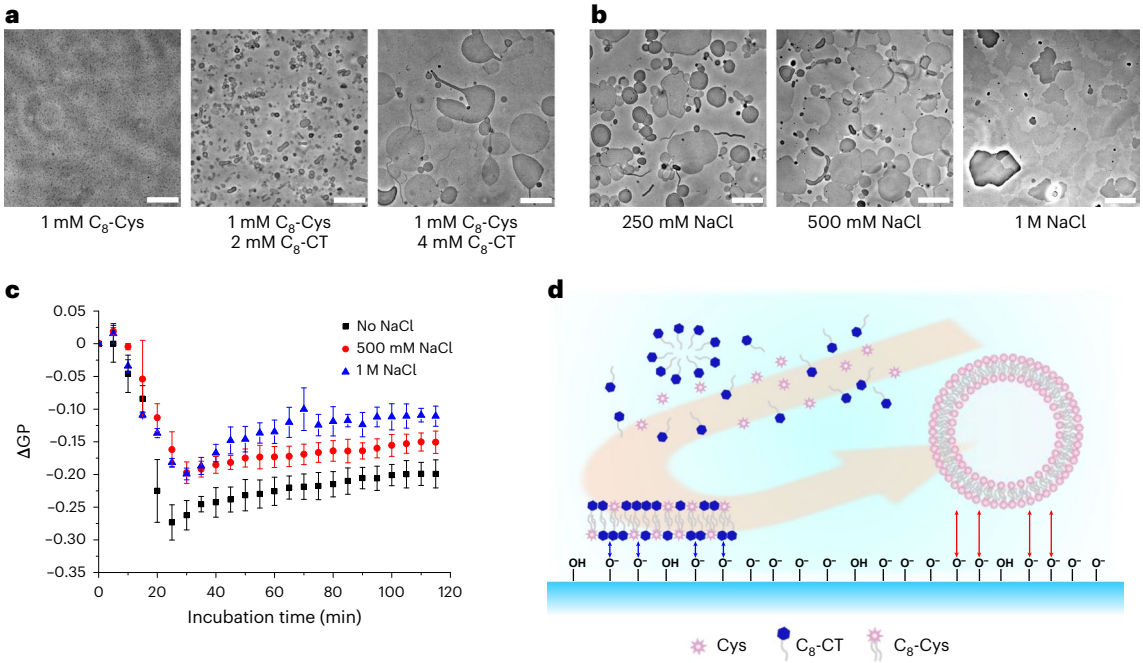

Fig. 3 | Mechanistic studies of silica surface-mediated formation of diacylcysteine vesicles. a, Film hydration of 1 mM C_8-Cys in 0.1 M, pH 8.0 sodium phosphate buffer at room teperature with or without additional C_8-CT. Phase-contrast microscopy images were obtained after 1 h incubation. **b**, Phase-contrast microscopy images of in situ C_8-Cys vesicle formation from a mixture of 1 mM Cys and 2 mM C_8-CT observed on the glass surface at various concentrations of NaCl. The phase-contrast microscopy images were obtained after 2 h incubation at room temperature. **c**, Change in Laurdan generalized polarization (ΔGP) during in situ C_8-Cys vesicle formation from 1 mM Cys and 2 mM C_8-CT on the glass surface at various concentrations of NaCl. The data points are presented as means ± s.d. ($n = 3$ technically independent samples). **d**, Schematic illustration of C_8-Cys vesicle formation on the glass surface. Electrostatic attraction and repulsion are indicated by blue and red arrows, respectively. Scale bars, 25 µm.

(ref. 29). The finding that C_8-Cys forms stable vesicles at submillimolar concentrations suggests that diacylcysteine species—if present on early Earth—would have been able to form membranes more readily than simple monocarboxylic acids.

We next determined how acyl chain length influences the reaction of thioesters with cysteine and protocell formation. Reactions between Cys and C_{12}-CT or $C_{14:1}$-CT afforded the corresponding diacylcysteine products under the same reaction conditions used to form C_8-Cys, and vesicle formation was also observed by microscopy (Supplementary Fig. 5c,d). However, no vesicles were detected when 2.5 mM Cys was incubated with 5 mM C_7-CT or C_6-CT, despite detection of the diacylated product by LCMS (Supplementary Fig. 6). Chemical synthesis of C_7-Cys and C_6-Cys allowed us to measure the critical aggregation concentrations of the diacylated products, which were 4.7 mM and 31.3 mM, respectively—much higher than that of C_8-Cys (Supplementary Fig. 8b,c). It therefore seems that thioesters with hydrophobic tails of at least eight carbons atoms are required to generate diacylcysteine vesicles using low millimolar concentrations of reactants.

Having explored the effect of lipid tail length on the formation of diacylcysteine vesicles, we performed similar experiments by attempting to vary the aminothiol lipid head group. Analogous to the results with Cys, 2-methylcysteine (2-Me-Cys) and homocysteine (HCy) were also diacylated by C_8-CT and the corresponding products formed vesicle structures at similar concentrations to C_8-Cys (Supplementary Fig. 5a,b). However, the formation of C_8-HCy was much slower than that of C_8-Cys, probably due to a less favourable S → N acyl transfer[39,40] (Supplementary Fig. 7).

For vesicles to function as protocells, they must be capable of carrying and retaining various biomolecules, including metabolic intermediates and genetic polymers. We therefore assessed the encapsulation capabilities of diacylcysteine vesicles. Using fluorescence microscopy, we found that C_8-Cys vesicles were able to retain small molecules such as the fluorescent dyes 8-hydroxypyrene-1,3,6-sulfonic acid (Fig. 1e and Supplementary Fig. 9a–c) and propidium iodide (Supplementary Fig. 9d–f), as well as large biomolecules such as the fluorescent protein sfGFP (Fig. 1f and Supplementary Fig. 9g–i).

Effect of solid substrates on diacylcysteine vesicle formation

As mentioned, during the reaction between 2.5 mM Cys and 5 mM C_8-CT, we noted the appearance of vesicles within 30 min. However, LCMS analysis of the reaction mixture indicated that only 0.2 mM of C_8-Cys had been formed, which is much lower than the measured critical aggregation concentration of 0.9 mM (Fig. 1b,c and Supplementary Fig. 8a). As vesicle formation was mostly observed at the glass cover-slip, we proceeded to examine the influence of the silica surface on vesicle assembly. Past reports have shown that the formation of prebiotic membranes can be greatly facilitated by solid supports such as silicate clays[35]. A solution of Cys and C_8-CT was directly mixed on a glass slide to a final concentration of 1 mM and 2 mM, respectively, and then immediately covered by a glass cover-slip (Fig. 2a). Phase-contrast microscopy and fluorescence microscopy using the fluorescent membrane-staining dye Nile Red revealed the formation of flattened lipid structures adsorbed to the glass cover-slip surface within 10 min of incubation, followed by vesicle formation. In addition to vesicle formation, over time we also observed several instances of vesicle growth and budding (Supplementary Fig. 10). However, under these conditions, only 0.05 mM of C_8-Cys was detected by LCMS after 1 h of incubation (Figs. 2b and 4b, and Supplementary Videos 1 and 2), further suggesting that the glass surface is playing a key role in membrane assembly. Consistent with our microscopy analysis, turbidity studies also revealed that C_8-Cys vesicle formation is facilitated by silica microspheres (Fig. 2c).

To better understand the role of the substrate, we chemically modified the cover-slip surface using different functional groups and performed in situ generation of C_8-Cys (Supplementary Fig. 13). Bare glass surfaces consist of silanol groups and are expected to be negatively charged in aqueous buffer. Interestingly, we observed the formation of

https://doi.org/10.1038/s41557-024-01666-y

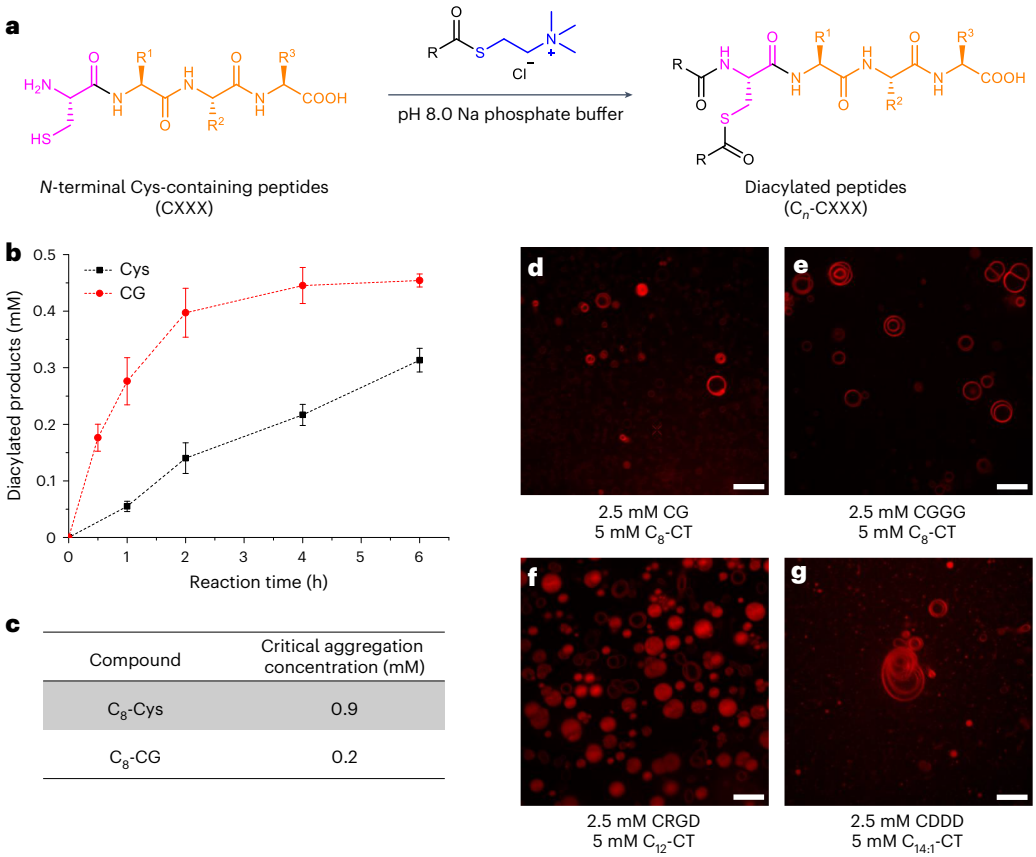

Fig. 4 | Vesicle formation by reaction of peptides and choline thioesters. **a**, General schematic for diacylation of *N*-terminal Cys-containing peptides. **b**, Reaction kinetics of the diacylation between 1 mM Cys or CG, and 2 mM C_8-CT (that is, Cys + C_8-CT and CG + C_8-CT, respectively). The products were quantified by LCMS, where the absorbance was monitored at 230 nm. The data points are presented as means ± s.d. (n = 3 technically independent samples). **c**, Critical aggregation concentrations of C_8-Cys and C_8-CG. **d**–**g**, Fluorescence microscopy images of representative diacylated peptide vesicles produced by in situ reactions in 0.1 M, pH 8.0 sodium phosphate buffer containing 1 μM Nile Red at room temperature (**d**, 2.5 mM CG + 5 mM C_8-CT after 5 h; **e**, 2.5 mM CGGG + 5 mM C_8-CT after 5 h; **f**, 2.5 mM CRGD + 5 mM C_{12}-CT after 2 h; **g**, 2.5 mM CDDD + 5 mM $C_{14:1}$-CT after 48 h). Scale bars, 25 μm.

distinct flattened lipid structures when reactions were performed on a positively charged (3-aminopropyl)triethoxysilane-modified (APTES) glass surface. However, no vesicular structures were detected on the glass or in the solution phase, even after 24 h of incubation (Fig. 2e and Supplementary Video 3). One possible explanation for this result is that the favourable electrostatic interactions between the positively charged amines on the glass surface and the negatively charged head group of the diacylcysteine product inhibits the detachment of membranes into solution. Conversely, membrane formation was inhibited when Cys and C_8-CT were incubated on a neutrally charged and hydrophobic C_{18}-modified glass surface (Fig. 2f and Supplementary Video 4).

After confirming that mixtures of 1 mM Cys and 2 mM C_8-CT lead to vesicle formation with the assistance of the unmodified glass surface, we determined whether using lower concentrations of the precursors would also result in the observation of vesicles. With 0.5 mM Cys and 1 mM C_8-CT, only small, flattened lipid structures adhered to the cover-slip were observed (Supplementary Fig. 14a). Surprisingly, simply increasing the concentration of C_8-CT to 2 mM led to the formation of vesicles (Supplementary Fig. 14b). Even, 0.25 mM Cys was sufficient for vesicle formation to occur with 2 mM C_8-CT (Supplementary Fig. 14c). Observing a critical role for the concentration of C_8-CT, we suspected that excess C_8-CT in the reaction mixture may co-assemble with synthesized C_8-Cys, resulting in the formation of mixed amphiphilic assemblies that could interact with the charged glass surface.

To test this hypothesis, we hydrated dried films of C_8-Cys doped with additional C_8-CT. As more C_8-CT was added, the size of the flattened structures also increased (Fig. 3a). On the other hand, when 1 mM C_8-Cys was incubated with either 4 mM octanoic acid or octanol, the results were similar to those obtained with C_8-Cys alone, further suggesting that favourable electrostatic interactions between the glass surface and mixed membranes are responsible for the observation of flattened membranes (Supplementary Fig. 15). Interestingly, the addition of 4 mM Cys to a mixture of 1 mM C_8-Cys and 4 mM C_8-CT resulted in the gradual decrease in both the size and population of the flattened structures (Supplementary Fig. 16), possibly due to consumption of the C_8-CT through diacylation.

If electrostatic interactions between the membrane and the glass surface play a critical role in vesicle formation, we would expect the ionic strength of the media to have a pronounced effect. We formed C_8-Cys vesicles by mixing 1 mM Cys and 2 mM C_8-CT on a glass surface at various concentrations of NaCl. As the ionic strength of the buffer increased, the number of vesicles decreased, and we observed more flattened lipid structures that were adhered to the glass surface. Strikingly, at 1 M NaCl, only flattened structures were observed (Figs. 2d and 3b, and Supplementary Videos 1 and 5–7). We also monitored the change in Laurdan generalized polarization (ΔGP) during membrane formation (Fig. 3c). It was evident that the decrease in GP was less pronounced at higher NaCl concentrations, indicating lower solvent penetration into the membrane at elevated ionic strengths, as would be expected for membrane structures tightly adsorbed to a surface[41]. According to past studies, it is generally regarded that as the ionic strength of the solvent increases, the electrostatic interaction between the membrane and the glass surface decreases, while van der Waals interactions become stronger[42,43]. Consequently, the

https://doi.org/10.1038/s41557-024-01666-y

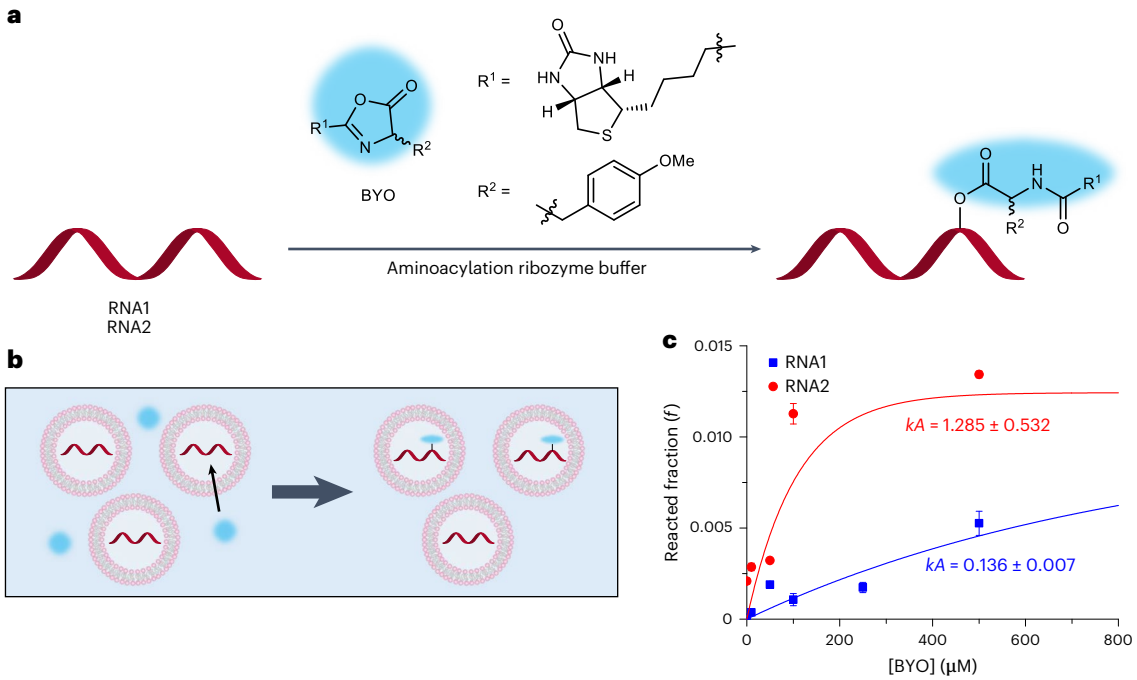

Fig. 5 | Ribozyme activity inside diacylcysteine vesicles. a, Reaction between self-aminoacylating ribozymes and biotinyl-Tyr(Me)-oxazolone (BYO). **b**, Schematic diagram of aminoacylation of the model ribozymes encapsulated inside the vesicles. **c**, The activities of ribozymes RNA1 (blue) and RNA2 (red) inside the mixed vesicles composed of C_8-Cys/C_{12}-*rac*-glycerol (1:0.5 molar ratio), as measured by RT–qPCR. The ribozyme-containing vesicles were extruded through polycarbonate membranes with pore sizes of 100 nm before addition of BYO. The reaction mixture—that is, 10 mM C_8-Cys, 5 mM C_{12}-*rac*-glycerol, 0.05 μM ribozyme and the indicated concentration of BYO—was incubated in the aminoacylation ribozyme buffer solution (0.1 M HEPES, 0.1 M KCl, 5 mM $MgCl_2$, pH 7.0) for 90 min. Ribozyme activities (*kA*) were determined by fitting data to a pseudo-first-order rate equation and are expressed in min^{-1} M^{-1} (Methods). The data points are presented as means ± s.d. ($n = 3$ technically independent samples).

dominant formation of flattened bilayers at high NaCl concentration conditions might originate from reduced electrostatic repulsion of the diacylcysteine head groups and the glass surface, along with increased van der Waals attractions. Furthermore, reactions in lower ionic strength media (10 mM sodium phosphate buffer) also resulted in vesicle formation, suggesting that C_8-Cys vesicles can be formed under conditions associated with natural sources of freshwater, such as lake water (Supplementary Video 8). Interestingly, we noted that detachment of the vesicles from the glass surface seems to be much faster when compared with the 100 mM sodium phosphate buffer conditions.

Taken together, we propose an electrostatic mechanism for vesicle formation through reaction between Cys and C_8-CT on glass surfaces (Fig. 3d). Initially formed C_8-Cys and remaining excess C_8-CT co-assemble on the glass surface, observed as flattened bilayer structures. Favourable electrostatic interactions and van der Waals attractions may lead to a high local concentration of C_8-Cys and C_8-CT on the surface, aiding C_8-Cys and membrane assembly even at concentrations under the critical aggregation concentration. Supporting this hypothesis is the lack of flattened structures during vesicle formation using negatively charged thioesters such as C_8-MESNA (Supplementary Fig. 3). As diacylation proceeds, the C_8-CT concentration decreases and the surface charge of the mixed membrane gets more negative due to the carboxylate head groups. The interaction between the membrane and the glass surface becomes less favourable, which eventually leads to release of the bilayer and vesicle assembly.

Formation of lipopeptide vesicles from *N*-terminal Cys-containing peptides

Recent studies have revealed prebiotically plausible synthetic routes to Cys-containing peptides[33]. We were curious as to whether C_8-CT-mediated diacylation was also feasible with *N*-terminal Cys-containing peptides, and whether the product lipids could assemble into giant vesicles (Fig. 4a). Incubation of 2.5 mM CG with 5 mM C_8-CT indeed resulted in spontaneous diacylation and vesicle formation (Fig. 4d and Supplementary Fig. 18a–c). We also extended the peptide length and attempted reactions using CGG and CGGG peptides, which afforded the corresponding diacylation products as well as vesicle formation (Fig. 4e, and Supplementary Figs. 17 and 18d–f). When 1 mM CG or CGGG peptide was incubated with 2 mM C_8-CT on a glass surface, rapid membrane formation on the surface, as well as vesicle formation in the solution phase, was observed by phase-contrast microscopy within 20 min of incubation (Supplementary Figs. 11 and 12). Interestingly, LCMS monitoring of the reactions revealed that the diacylation of CG is much faster than that of Cys (Fig. 4b). Additionally, the critical aggregation concentration of C_8-CG (0.2 mM) was lower than that of C_8-Cys (Fig. 4c and Supplementary Fig. 8d). This might be attributed to hydrogen bonding between adjacent peptides in the lipopeptide membrane and the hydrophobic nature of the additional glycine backbone. It is tempting to speculate that protocells consisting of simple C_8-Cys lipids may have had a selection pressure to evolve catalysts to drive peptide bond formation, which would have provided a competitive advantage through stabilization of the membrane compartment.

Encouraged by these results, we envisaged that peptides with more complex sequences might similarly produce vesicles. Notably, three different *N*-terminal Cys-containing peptides—CRGD, CDDD and CDGR—underwent similar diacylation and vesicle formation with choline thioesters, although they required slightly longer hydrophobic tails (C_{12} for CRGD, and $C_{14:1}$ for CDDD and CDGR), probably due to their larger hydrophilic head groups, which would be expected to result in a decrease in the packing parameter (Fig. 4f,g, and Supplementary Figs. 18g–l and 19). These findings suggest that primordial vesicles composed of diacylcysteine derivatives might have been able to exhibit a range of structural configurations and increased functional variety

compared with simple fatty acids and phospholipids, which may have been necessary before the evolution of more advanced transmembrane proteins.

Ribozyme activity inside diacylcysteine vesicles

A major drawback of fatty-acid-based vesicles is their instability in the presence of divalent cations[4–7,19,20]. The RNA world hypothesis is accepted as one of the most plausible scenarios for the origin of life, as RNA can act as both a genetic material and catalyst. It is hypothesized that self-replicating RNA molecules may have served as the first genetic material on early Earth[44]. Given that divalent cations are required for the function of ribozymes, it is reasonable that protocells would have needed to be stable in the presence of these cations. We therefore evaluated the stability of the diacylcysteine vesicles in sodium phosphate buffer comprising Mg^{2+} or Ca^{2+} ions at concentrations that are thought to be relevant to prebiotic environments and would support ribozyme function. We found that C_8-Cys vesicles remained stable in the presence of 2 mM Ca^{2+} (Supplementary Fig. 20a) but lost their structure when exposed to 10 mM Ca^{2+} (Supplementary Fig. 20b). Furthermore, the vesicles remained stable when exposed to 10 mM Mg^{2+} (Supplementary Fig. 20d). Moreover, we found that C_8-Cys vesicles can be spontaneously generated by diacylation in buffer containing 5 mM Mg^{2+} and up to 2 mM Ca^{2+} (Supplementary Fig. 21). Overall, our results demonstrate that C_8-Cys vesicles exhibit much higher stability to divalent cations than vesicles composed of only fatty acids[20].

To explore whether ribozyme activity could be sustained within C_8-Cys vesicles, we encapsulated recently discovered aminoacylating ribozymes RNA1 and RNA2 (ref. 45) (Fig. 5a). Size-exclusion column chromatography and centrifugation were used to separate vesicles containing ribozymes from unencapsulated ribozymes, and we found that pure C_8-Cys vesicles were mechanically fragile during this process. As such, mixed vesicles composed of C_8-Cys and simple monoacylglycerols were prepared to enhance vesicle stability[24,46]. We found that the mixed vesicles composed of C_8-Cys and C_{12}-*rac*-glycerol in a 1:0.5 molar ratio exhibited sufficient stability for purification (Supplementary Figs. 22–25).

Self-aminoacylating ribozymes were encapsulated inside mixed vesicles composed of C_8-Cys and C_{12}-*rac*-glycerol (1:0.5 molar ratio) followed by purification to eliminate unencapsulated ribozyme (Fig. 5b). The acylation substrate biotinyl-Tyr(Me)-oxazolone (BYO) was then added to the reaction mixture. After 90 min of incubation, the aminoacylated RNA product was measured by quantitative polymerase chain reaction with reverse transcription (RT–qPCR), and formation of the desired aminoacylated product was evident (Fig. 5c). Thus, C_8-Cys/C_{12}-*rac*-glycerol vesicles permit entry of the BYO substrate while keeping the encapsulated RNAs within the vesicles. Catalysis also took place using unencapsulated ribozymes in the presence of vesicles (Supplementary Fig. 26). These results demonstrate that diacylated cysteine vesicles are compatible with functional ribozymes, and suggest a potential link between membrane formation and cellular functionality.

Conclusion

In this study we investigated spontaneous formation of diacylcysteine vesicles from Cys and short-chain choline thioesters. C_8-Cys was found to be capable of vesicle formation even at submillimolar concentrations. Furthermore, the real-time observation of C_8-Cys vesicle formation suggests that the initial formation and growth of the vesicles takes place at the glass surface, even when the bulk concentration of C_8-Cys is much lower than the critical aggregation concentration. We found evidence suggesting that electrostatic interactions between lipid membranes and the silica substrate play a crucial role in vesicle assembly. The rapid reaction kinetics and silica-substrate-templated vesicle formation enabled the generation of diacylcysteine vesicles at low effective concentrations of precursors. In addition to Cys, *N*-terminal Cys-containing peptides similarly reacted with choline thioesters to generate vesicles, expanding the compositional diversity of diacylcysteine-based lipid structures. Finally, diacylcysteine vesicles remained stable in the presence of divalent cations at concentrations appropriate for ribozyme activity, and self-aminoacylating ribozymes were shown to be active inside diacylcysteine vesicles. Overall, our work demonstrates that reactions between simple precursors in water can yield diacyl amphiphiles that assemble into giant vesicles, expanding the possible routes by which protocell membrane formation can occur.

Online content

Any methods, additional references, Nature Portfolio reporting summaries, source data, extended data, supplementary information, acknowledgements, peer review information; details of author contributions and competing interests; and statements of data and code availability are available at https://doi.org/10.1038/s41557-024-01666-y.

References

1. Devaraj, N. K. In situ synthesis of phospholipid membranes. *J. Org. Chem.* **82**, 5997–6005 (2017).
2. Dowhan, W. A retrospective: use of *Escherichia coli* as a vehicle to study phospholipid synthesis and function. *Biochim. Biophys. Acta* **1831**, 471–494 (2013).
3. Vance, J. E. Phospholipid synthesis and transport in mammalian cells. *Traffic* **16**, 1–18 (2015).
4. Deamer, D. The role of lipid membranes in life's origin. *Life* **7**, 5 (2017).
5. Luisi, P. L., Walde, P. & Oberholzer, T. Lipid vesicles as possible intermediates in the origin of life. *Curr. Opin. Colloid Interface Sci.* **4**, 33–39 (1999).
6. Chen, I. A. & Walde, P. From self-assembled vesicles to protocells. *Cold Spring Harb. Perspect. Biol.* **2**, 1–13 (2010).
7. Szostak, J. W., Bartel, D. P. & Luisi, P. L. Synthesizing life. *Nature* **409**, 387–390 (2001).
8. Zepik, H. H., Walde, P. & Ishikawa, T. Vesicle formation from reactive surfactants. *Angew. Chem. Int. Ed.* **47**, 1323–1325 (2008).
9. Huang, Y. et al. Molecular and compound-specific isotopic characterization of monocarboxylic acids in carbonaceous meteorites. *Geochim. Cosmochim. Acta* **69**, 1073–1084 (2005).
10. Yuen, G. U. & Kvenvolden, K. A. Monocarboxylic acids in Murray and Murchison carbonaceous meteorites. *Nature* **246**, 301–303 (1973).
11. Mccollom, T. M., Ritter, G. & Simoneit, B. R. T. Lipid synthesis under hydrothermal conditions by Fischer–Tropsch-type reactions. *Orig. Life Evol. Biosph.* **29**, 153–166 (1999).
12. Lai, J. C.-Y., Pearce, B. K. D., Pudritz, R. E. & Lee, D. Meteoritic abundances of fatty acids and potential reaction pathways in planetesimals. *Icarus* **319**, 685–700 (2019).
13. Wang, A. & Szostak, J. W. Lipid constituents of model protocell membranes. *Emerg. Top. Life. Sci.* **3**, 537–542 (2019).
14. Monnard, P.-A. & Deamer, D. W. Membrane self-assembly processes: steps toward the first cellular life. *Anat. Rec.* **268**, 196–207 (2002).
15. Deamer, D. W. Boundary structures are formed by organic components of the Murchison carbonaceous chondrite. *Nature* **317**, 792–794 (1985).
16. Budin, I., Bruckner, R. J. & Szostak, J. W. Formation of protocell-like vesicles in a thermal diffusion column. *J. Am. Chem. Soc.* **131**, 9628–9629 (2009).
17. Budin, I., Debnath, A. & Szostak, J. W. Concentration-driven growth of model protocell membranes. *J. Am. Chem. Soc.* **134**, 20812–20819 (2012).
18. Budin, I., Prywes, N., Zhang, N. & Szostak, J. W. Chain-length heterogeneity allows for the assembly of fatty acid vesicles in dilute solutions. *Biophys. J.* **107**, 1582–1590 (2014).

19. Apel, C. L., Deamer, D. W. & Mautner, M. N. Self-assembled vesicles of monocarboxylic acids and alcohols: conditions for stability and for the encapsulation of biopolymers. *Biochim. Biophys. Acta* **1559**, 1–9 (2002).
20. Monnard, P.-A., Apel, C. L., Kanavarioti, A. & Deamer, D. W. Influence of ionic inorganic solutes on self-assembly and polymerization processes related to early forms of life: implications for a prebiotic aqueous medium. *Astrobiology* **2**, 139–152 (2002).
21. Namani, T. & Deamer, D. W. Stability of model membranes in extreme environments. *Orig. Life. Evol. Biosph.* **38**, 329–341 (2008).
22. Jordan, S. F. et al. Promotion of protocell self-assembly from mixed amphiphiles at the origin of life. *Nat. Ecol. Evol.* **3**, 1705–1714 (2019).
23. Maurer, S. E. et al. Vesicle self-assembly of monoalkyl amphiphiles under the effects of high ionic strength, extreme pH, and high temperature environments. *Langmuir* **34**, 15560–15568 (2018).
24. Maurer, S. E., Deamer, D. W., Boncella, J. M. & Monnard, P.-A. Chemical evolution of amphiphiles: glycerol monoacyl derivatives stabilize plausible prebiotic membranes. *Astrobiology* **9**, 979–987 (2009).
25. Ourisson, G. & Nakatani, Y. The terpenoid theory of the origin of cellular life: the evolution of terpenoids to cholesterol. *Chem. Biol.* **1**, 11–23 (1994).
26. Plobeck, N., Eifler, S., Brisson, A., Nakatani, Y. & Ourisson, G. Sodium di-polyprenyl phosphates form "primitive" membranes. *Tetrahedron Lett.* **33**, 5249–5252 (1992).
27. Griffith, E. C., Rapf, R. J., Shoemaker, R. K., Carpenter, B. K. & Vaida, V. Photoinitiated synthesis of self-assembled vesicles. *J. Am. Chem. Soc.* **136**, 3784–3787 (2014).
28. Gibard, C., Bhowmik, S., Karki, M., Kim, E.-K. & Krishnamurthy, R. Phosphorylation, oligomerization and self-assembly in water under potential prebiotic conditions. *Nat. Chem.* **10**, 212–217 (2018).
29. Bonfio, C. et al. Length-selective synthesis of acylglycerol-phosphates through energy-dissipative cycling. *J. Am. Chem. Soc.* **141**, 3934–3939 (2019).
30. Pulletikurti, S., Veena, K. S., Yadav, M., Deniz, A. A. & Krishnamurthy, R. Experimentally modeling the emergence of prebiotically plausible phospholipid vesicles. *Chem* **10**, 1839–1867 (2024).
31. Brea, R. J., Cole, C. M. & Devaraj, N. K. In situ vesicle formation by native chemical ligation. *Angew. Chem. Int. Ed.* **53**, 14102–14105 (2014).
32. Brea, R. J., Rudd, A. K. & Devaraj, N. K. Nonenzymatic biomimetic remodeling of phospholipids in synthetic liposomes. *Proc. Natl Acad. Sci. USA* **113**, 8589–8594 (2016).
33. Foden, C. S. et al. Prebiotic synthesis of cysteine peptides that catalyze peptide ligation in neutral water. *Science* **370**, 865–869 (2020).
34. Liu, L. et al. Enzyme-free synthesis of natural phospholipids in water. *Nat. Chem.* **12**, 1029–1034 (2020).
35. Hanczyc, M. M., Fujikawa, S. M. & Szostak, J. W. Experimental models of primitive cellular compartments: encapsulation, growth, and division. *Science* **302**, 618–622 (2003).
36. Steinman, G., Kenyon, D. H. & Calvin, M. Dehydration condensation in aqueous solution. *Nature* **206**, 707–708 (1965).
37. Flores, J. et al. Rapid and sequential dual oxime ligation enables de novo formation of functional synthetic membranes from water-soluble precursors. *Angew. Chem. Int. Ed.* **61**, e202200549 (2022).
38. Wilcoxen, K. M., Leman, L. J., Weinberger, D. A., Huang, Z.-Z. & Ghadiri, M. R. Biomimetic catalysis of intermodular aminoacyl transfer. *J. Am. Chem. Soc.* **129**, 748–749 (2007).
39. Canne, L. E., Bark, S. J. & Kent, S. B. H. Extending the applicability of native chemical ligation. *J. Am. Chem. Soc.* **118**, 5891–5896 (1996).
40. Lv, H. et al. Native chemical ligation combined with spirocyclization of benzopyrylium dyes for the ratiometric and selective fluorescence detection of cysteine and homocysteine. *Anal. Chem.* **86**, 1800–1807 (2014).
41. Boyd, M. A. & Kamat, N. P. Visualizing tension and growth in model membranes using optical dyes. *Biophys. J.* **115**, 1307–1315 (2018).
42. Richter, R. P., Bérat, R. & Brisson, A. R. Formation of solid-supported lipid bilayers: an integrated view. *Langmuir* **22**, 3497–3505 (2006).
43. Cremer, P. S. & Boxer, S. G. Formation and spreading of lipid bilayers on planar glass supports. *J. Phys. Chem. B* **103**, 2554–2559 (1999).
44. Higgs, P. G. & Lehman, N. The RNA world: molecular cooperation at the origins of life. *Nat. Rev. Genetics* **16**, 7–17 (2015).
45. Lai, Y.-C., Liu, Z. & Chen, I. A. Encapsulation of ribozymes inside model protocells leads to faster evolutionary adaptation. *Proc. Natl Acad. Sci. USA* **118**, e2025054118 (2021).
46. Chen, I. A., Roberts, R. W. & Szostak, J. W. The emergence of competition between model protocells. *Science* **305**, 1474–1476 (2004).

Publisher's note Springer Nature remains neutral with regard to jurisdictional claims in published maps and institutional affiliations.

Springer Nature or its licensor (e.g. a society or other partner) holds exclusive rights to this article under a publishing agreement with the author(s) or other rightsholder(s); author self-archiving of the accepted manuscript version of this article is solely governed by the terms of such publishing agreement and applicable law.

© The Author(s), under exclusive licence to Springer Nature Limited 2024

Methods

Vesicle formation from diacylcysteines and their analogues

Stock solution A: 5 mM Cys (or its analogue) in 0.1 M, pH 8.0 sodium phosphate buffer containing 10 mM tris(2-carboxyethyl)phosphine (TCEP)·HCl.

Stock solution B: 10 mM C_8-CT (or C_8-MESNA) in 0.1 M, pH 8.0 sodium phosphate buffer containing 10 mM TCEP·HCl.

Stock solutions A and B were prepared right before the experiment. Stock solution B (100 µl) was added to stock solution A (100 µl) in a glass vial and then the reaction mixture was tumbled at room temperature (final concentration of Cys (or its analogue) = 2.5 mM; C_8-CT (or C_8-MESNA) = 5 mM). After the indicated time points in Fig. 1b, 2 µl of the reaction mixture was dispensed on a glass slide and covered with a glass cover-slip; the phase-contrast microscopy images were then obtained.

Reaction kinetics of diacylation

Stock solution A: 5 mM (or 2 mM) Cys (or its analogue) in 0.1 M, pH 8.0 sodium phosphate buffer containing 10 mM (or 4 mM) TCEP·HCl.

Stock solution B: 10 mM (or 4 mM) C_8-CT (or C_8-MESNA) in 0.1 M, pH 8.0 sodium phosphate buffer containing 10 mM (or 4 mM) TCEP·HCl.

Stock solutions A and B were prepared right before the experiment. Stock solution B (500 µl) was added to stock solution A (500 µl) in a glass vial and then the reaction mixture was tumbled at room temperature. After the indicated time points in Figs. 1c and 4b, and Supplementary Fig. 7, 80 µl of the reaction mixture was diluted with 240 µl MeOH and then filtered through a 0.45 µm polytetrafluoroethylene filter. The amount of the diacylated product was measured by LCMS analysis using 230 nm ultraviolet absorbance on the basis of the calibration curve created using a chemically synthesized authentic sample.

Determination of the critical aggregation concentration

Critical aggregation concentration of diacylcysteines and diacylated lipopeptide was determined following a procedure reported in the literature[34]. Thin films of diacylcysteines and diacylated peptides were prepared by dissolving 0.1–3.0 mg of the compounds in a glass vial using a minimal amount of chloroform, which was then evaporated by blowing it with argon gas. The films were further dried in air at room temperature for several hours. The diacylcysteine or diacylated peptide solutions with the indicated concentrations were then prepared by film hydration in 0.1 M, pH 8.0 sodium phosphate buffer. The resulting samples were allowed to equilibrate for 30 min, after which 0.4 µl of a 2.5 mM Laurdan solution in EtOH was added to 400 µl of each sample and then gently mixed; 20 µl of each sample was then transferred to a 384-well plate and analysed on a Tecan Infinite plate reader. The samples were excited at 364 nm and emission spectra were acquired over 400–600 nm. The generalized polarization (GP) was calculated as follows:

$$\mathrm{GP} = \frac{I_{440} - I_{490}}{I_{440} + I_{490}}$$

In situ vesicle formation on solid substrates

Stock solution A: 2 mM Cys (or its analogue) in 0.1 M, pH 8.0 sodium phosphate buffer containing 4 mM TCEP·HCl.

Stock solution B: 4 mM C_8-CT (or C_8-MESNA) in 0.1 M, pH 8.0 sodium phosphate buffer containing 4 mM TCEP·HCl.

Stock solutions A and B were prepared right before the experiment; 2 µl of stock solution A was carefully pipetted onto a glass (or chemically modified) slide, followed by addition of 2 µl of stock solution B. The solution was gently mixed by upwards and downwards pipetting, and then covered with a glass (or chemically modified) cover-slip. The resulting mixture was monitored by phase-contrast or fluorescence microscopy to analyse the in situ formation and growth of the vesicles (final concentration of Cys (or its analogue) = 1 mM; C_8-CT (or C_8-MESNA) = 2 mM).

Turbidity monitoring during in situ C_8-Cys vesicle formation with and without silica microspheres

Stock solution A: 2 mM Cys in 0.1 M, pH 8.0 sodium phosphate buffer containing 4 mM TCEP·HCl.

Stock solution B: 4 mM C_8-CT and 5 µm silica microsphere at twice of the indicated final concentration in 0.1 M, pH 8.0 sodium phosphate buffer containing 4 mM TCEP·HCl.

Stock solutions A and B were prepared right before the experiment. Stock solution B (850 µl) was added to stock solution A (850 µl) in a 2 ml Eppendorf tube, and then the reaction mixture was gently vortexed for a few seconds; 1.5 ml of the mixture was then transferred to a polystyrene cuvette equipped with a magnetic stir bar and the mixture was stirred at room temperature (final concentration of Cys = 1 mM; C_8-CT = 2 mM). Turbidity was measured at 400 nm every 2 min for a period of 2 h using a NanoDrop 2000c spectrophotometer.

Evaluation of ribozyme activity in vesicles

Preparation of the mixed vesicles of C_8-Cys and C_{12}-*rac*-glycerol. A 1:0.5 molar ratio mixture of C_8-Cys and C_{12}-*rac*-glycerol in MeOH/chloroform (v/v 2:1) was added to a glass vial, and then a dry thin film was prepared by gently blowing argon over the mixture. The film was further dried under vacuum for 12 h and then hydrated by addition of aminoacylation ribozyme buffer without $MgCl_2$ (0.1 M HEPES, 0.1 M NaCl, 0.1 M KCl, pH 7.0) (final concentration of C_8-Cys = 50 mM). The resulting mixture was tumbled at room temperature overnight and then extruded through polycarbonate membranes with pore sizes of 100 nm (Whatman) using a lipid extruder (Avanti Polar Lipids, catalogue number 61000).

Preparation of the ribozymes. All DNA molecules were chemically synthesized and polyacrylamide gel electrophoresis (PAGE)-purified from Integrated DNA Technologies. The template DNA molecules with the sequence 5′-GATAATACGACTCACTATAGGGAATGGATCCACATCTACGAATTC-N21-TTCACTGCAGACTTGACGAAGCTG-3′; the nucleotides upstream of the transcription start site for T7 RNA polymerase are underlined, and N21 denotes 21 consecutive nucleotides, which are CTACTTCAAACAATCG-GTCTG for RNA1 and ATTACCCTGGTCATCGAGTGA for RNA2. RNAs were transcribed using HiScribe T7 polymerase (New England Biolabs) and purified by denaturing polyacrylamide gel electrophoresis (National Diagnostics).

Preparation of vesicle-encapsulated ribozymes and ribozymes exposed to empty vesicles. To prepare vesicles encapsulating ribozymes[45], RNAs were added into the aminoacylation ribozyme buffer without $MgCl_2$ (0.1 M HEPES, 0.1 M NaCl, 0.1 M KCl, pH 7.0) and incubated overnight with the dried lipid films, followed by extrusion as above. The RNA amount before the encapsulation was 48 µg. After extrusion, 5 mM $MgCl_2$ was added into the liposome solution and incubated for 30 min. The RNA-containing vesicles were purified using a Sepharose 4B size-exclusion column (Sigma-Aldrich), with the aminoacylation buffer (0.1 M HEPES, 0.1 M NaCl, 0.1 M KCl, 5 mM $MgCl_2$, pH 7.0) as the mobile phase to remove unencapsulated RNAs. The purified RNA-containing vesicles were concentrated by a 50 kDa MWCO Amicon Ultra-4 centrifugal filter unit (Millipore Sigma). The final RNA concentration of samples before BYO incubation was about 0.05 µM.

To prepare non-encapsulated RNA exposed to empty vesicles[45], 5 mM $MgCl_2$ was added to the extruded liposome solution, which was then equilibrated for 30 min, followed by the addition of the RNA solution. The final RNA concentration of samples before the BYO incubation was 0.5 µM. The final concentration of the C_8-Cys/C_{12}-*rac*-glycerol mixed vesicle was 50 mM, on the basis of that of C_8-Cys.

Note that the purification of the ribozyme-encapsulating vesicles dilutes the vesicles by approximately a factor of five. Thus, the final concentration of the vesicles was estimated as 10 mM on the basis of the amount of initial C_8-Cys. Following the calculation demonstrated in

the literature[47], and with an assumption that a membrane surface area is approximately 0.5 nm^2 per lipid[47], the total surface area of a 10 mM lipid solution would be 150 $m^2\ l^{-1}$. A single 100-nm-sized vesicle would have a surface area of 1.3×10^{-13} m^2, and so we estimate there are approximately 10^{15} vesicles per litre. Furthermore, the final RNA concentration in the vesicles was 50 nM (3×10^{16} molecules per litre) after purification. By dividing the RNA concentration by the vesicle concentration, it is therefore calculated that there are approximately 30 RNA molecules per vesicle.

Experimental measurement of ribozyme activity by RT–qPCR. The activities of selected ribozymes were determined by RT–qPCR, as previously described in ref. 45. DNA sequences were chemically synthesized and PAGE-purified by Integrated DNA Technologies. The synthesized DNA sequences were 5′-GATAATACGACTCACTATAGGGAATGGATCCACATCTACGAATTC-N21-TTCACTGCAGACTTGACGAAGCTG-3′; the nucleotides upstream of the transcription start site for T7 RNA polymerase are underlined, and N21 denotes 21 consecutive nucleotides, which are CTACTTCAAACAATCGGTCTG for RNA1 and ATTACCCTGGTCATCGAGTGA for RNA2. RNAs were transcribed using HiScribe T7 polymerase (New England Biolabs) and purified by denaturing PAGE (National Diagnostics). The ribozyme samples—encapsulated inside or non-encapsulated in vesicles—were prepared as described above and incubated for 90 min with various BYO substrate concentrations (10, 50, 100, 250, 500 and 1,000 μM) in a total volume of 50 μl for each sample. The reactions were stopped by removing unreacted substrate using Bio-Spin P-30 Tris-desalting columns (Bio-Rad). The RNA concentration of each sample was quantified by a QubitR 3.0 Fluorometer (Thermo-Fisher Scientific). To isolate the reacted RNA, 20 μl (1 mg ml^{-1}) of streptavidin MagneSphere paramagnetic beads (Promega) was added to all of the reacted RNA samples (20 ng RNA for each sample from the dissolved reacted RNA stock solutions). Samples were incubated for 10 min at room temperature with end-over-end tumbling, followed by three washing steps. The aminoacylated RNAs were eluted with UltraPure DEPC-Treated Water (Invitrogen) incubated at 70 °C for 1 min. The amounts of aminoacylated RNAs were quantified using iTaq SYBR green mix (catalogue number 1725150, Bio-Rad) using a Bio-Rad CFX96 Touch system. The samples were prepared following the manufacturer's protocol: 2 μl samples were mixed in the total 10 μl RT–qPCR reaction volume with 500 nM of both forward and reverse primers. The forward and reverse primers sequence were 5′-GATAATACGACTCACTATAGGGAATGGATCCACATCTACGA-3′ and 5′-CAGCTTCGTCAAGTCTGCAGTGAA-3′, respectively. A calibration standard curve was measured for each RT–qPCR measurement batch to reduce measurement error. The standard RNA sequence was 5′-GGGAAUGGAUCCACAUCUACGAAUUCAAAAACAAAAACAAAAACAAANUUCACUGCAGACUUGACGAAGCUG-3′, which has the same length (that is, 71 bp) and primer-complementary regions as the ribozymes used in this study. The standard curve was determined by adding 2 μl standard RNA samples with the concentrations of 1,000, 100, 10, 1 and 0.1 pg μl^{-1}. Triplicates were performed for each sample. Results were fit to the pseudo-first-order rate equation $F = A(1 - e^{-k[BYO]t})$, where F is the reacted fraction, A is the maximum reacted fraction, t is the incubation time of 90 min and k is the effective rate constant of the aminoacylation reaction. The two fitting parameters A and k are poorly estimated individually for low-activity sequences (approximately $k < 0.5\ min^{-1}\ M^{-1}$), but due to the inverse correlation between estimated A and k during curve fitting, the product of the estimated k and estimated A is more accurate[48]. Therefore, the product of the two estimated parameters, kA, from the pseudo-first-order curve fitting, was used to represent the catalytic activity of ribozymes in the present study.

Statistics and reproducibility. Each experiment in Figs. 1d–f, 2d–f and 4d–g, and Supplementary Figs. 3–5, 9–12, 14, 15 and 17–25 was repeated independently at least three times, with similar results.

Reporting summary

Further information on research design is available in the Nature Portfolio Reporting Summary linked to this article.

Data availability

All data are available in the main text or Supplementary Information. Source Data are provided with this paper.

References

47. Brügger, B. et al. The HIV lipidome: a raft with an unusual composition. *Proc. Natl Acad. Sci. USA* **103**, 2641–2646 (2006).
48. Shen, Y., Pressman, A., Janzen, E. & Chen, I. A. Kinetic sequencing (k-seq) as a massively parallel assay for ribozyme kinetics: utility and critical parameters. *Nucleic Acids Res.* **49**, e67 (2021).

Acknowledgements

N.K.D. and I.A.C. acknowledge support from the National Science Foundation (grant no. EF-1935372). N.K.D. acknowledges support from the National Institutes of Health (grant no. R35-GM141939). I.A.C. acknowledges support from NASA (grant no. 80NSSC21K0595). We thank I. Budin for helpful discussions and feedback on this paper, and W. Hoi for his help with the cryo-EM data collection at the Electron Imaging Center for Nanomachines (EICN) at the California NanoSystems Institute (CNSI) at UCLA. The funders had no role in study design, data collection and analysis, decision to publish or preparation of the manuscript.

Author contributions

N.K.D., C.J.C. and T.A. conceived the research. C.J.C., T.A., I.A.C. and N.K.D. designed the experiments. C.J.C., T.A., Y.-C.L., A.V.-S., A.F. and R.J.B. performed experiments and analysed the data. C.J.C., T.A., I.A.C. and N.K.D. wrote the paper. C.J.C. and T.A. contributed equally to this work. All authors discussed the results and commented on the paper.

Competing interests

The authors declare no competing interests.

Additional information

Supplementary information The online version contains supplementary material available at https://doi.org/10.1038/s41557-024-01666-y.

Correspondence and requests for materials should be addressed to Neal K. Devaraj.

Peer review information *Nature Chemistry* thanks Sarah Maurer and the other, anonymous, reviewer(s) for their contribution to the peer review of this work.

Reprints and permissions information is available at www.nature.com/reprints.

nature portfolio

Corresponding author(s): Neal K. Devaraj

Last updated by author(s): Jul 26, 2024

Reporting Summary

Nature Portfolio wishes to improve the reproducibility of the work that we publish. This form provides structure for consistency and transparency in reporting. For further information on Nature Portfolio policies, see our Editorial Policies and the Editorial Policy Checklist.

Statistics

For all statistical analyses, confirm that the following items are present in the figure legend, table legend, main text, or Methods section.

n/a	Confirmed	
☐	☒	The exact sample size (*n*) for each experimental group/condition, given as a discrete number and unit of measurement
☐	☒	A statement on whether measurements were taken from distinct samples or whether the same sample was measured repeatedly
☒	☐	The statistical test(s) used AND whether they are one- or two-sided *Only common tests should be described solely by name; describe more complex techniques in the Methods section.*
☒	☐	A description of all covariates tested
☒	☐	A description of any assumptions or corrections, such as tests of normality and adjustment for multiple comparisons
☐	☒	A full description of the statistical parameters including central tendency (e.g. means) or other basic estimates (e.g. regression coefficient) AND variation (e.g. standard deviation) or associated estimates of uncertainty (e.g. confidence intervals)
☒	☐	For null hypothesis testing, the test statistic (e.g. *F*, *t*, *r*) with confidence intervals, effect sizes, degrees of freedom and *P* value noted *Give P values as exact values whenever suitable.*
☒	☐	For Bayesian analysis, information on the choice of priors and Markov chain Monte Carlo settings
☒	☐	For hierarchical and complex designs, identification of the appropriate level for tests and full reporting of outcomes
☒	☐	Estimates of effect sizes (e.g. Cohen's *d*, Pearson's *r*), indicating how they were calculated

Our web collection on statistics for biologists contains articles on many of the points above.

Software and code

Policy information about availability of computer code

Data collection	No software was used.
Data analysis	No software was used.

For manuscripts utilizing custom algorithms or software that are central to the research but not yet described in published literature, software must be made available to editors and reviewers. We strongly encourage code deposition in a community repository (e.g. GitHub). See the Nature Portfolio guidelines for submitting code & software for further information.

Data

Policy information about availability of data

All manuscripts must include a data availability statement. This statement should provide the following information, where applicable:

- Accession codes, unique identifiers, or web links for publicly available datasets
- A description of any restrictions on data availability
- For clinical datasets or third party data, please ensure that the statement adheres to our policy

The authors declare that the data supporting the findings of this study are available within the paper and its Supplementary Information files.

Human research participants

Policy information about studies involving human research participants and Sex and Gender in Research.

Reporting on sex and gender	Not applicable.
Population characteristics	Not applicable.
Recruitment	Not applicable.
Ethics oversight	Not applicable.

Note that full information on the approval of the study protocol must also be provided in the manuscript.

Field-specific reporting

Please select the one below that is the best fit for your research. If you are not sure, read the appropriate sections before making your selection.

☒ Life sciences ☐ Behavioural & social sciences ☐ Ecological, evolutionary & environmental sciences

For a reference copy of the document with all sections, see nature.com/documents/nr-reporting-summary-flat.pdf

Life sciences study design

All studies must disclose on these points even when the disclosure is negative.

Sample size	Not applicable.
Data exclusions	No data were excluded from the analyses.
Replication	All attempts at replication were successful.
Randomization	Not applicable.
Blinding	Not applicable.

Reporting for specific materials, systems and methods

We require information from authors about some types of materials, experimental systems and methods used in many studies. Here, indicate whether each material, system or method listed is relevant to your study. If you are not sure if a list item applies to your research, read the appropriate section before selecting a response.

Materials & experimental systems

n/a	Involved in the study
☒	☐ Antibodies
☒	☐ Eukaryotic cell lines
☒	☐ Palaeontology and archaeology
☒	☐ Animals and other organisms
☒	☐ Clinical data
☒	☐ Dual use research of concern

Methods

n/a	Involved in the study
☒	☐ ChIP-seq
☒	☐ Flow cytometry
☒	☐ MRI-based neuroimaging